The Island Arc (1996) **5**, 373–385

Research Article

Thermal evolution of the Ryoke metamorphic belt, southwestern Japan: Tectonic and numerical modeling

TAKAMOTO OKUDAIRA*

Department of Earth and Planetary Systems Science, Faculty of Science, Hiroshima University, 1-3-1 Kagamiyama, Higashi-Hiroshima 739, Japan

Abstract The Ryoke metamorphic belt of southwestern Japan is composed of Cretaceous Ryoke granitoids and associated metamorphic rocks of low-pressure facies series. The Ryoke granitoids are divided into sheet-like bodies (e.g. Gamano granodiorite) and stock-like bodies. The Gamano granodiorite intruded concordantly into the high-grade metamorphic rocks without development of a contact metamorphic aureole, and the intrusion ages of the granodiorite are similar to the ages of thermal peak of the low pressure (low-P) metamorphism. It is suggested that the low-P Ryoke metamorphism resulted from the intrusion of the Gamano granodiorite. In this study, a simple 1-D numerical model of conductive heat transfer was used to evaluate the thermal effects of emplacement of the Gamano granodiorite. Calculated temperature-time (T–t) paths are characterized by a rapid increase of metamorphic temperature and a relatively short-lived period of high temperature. For example, the T–t path at the 15-km depth is characterized by a rapid average increase in temperature of 1.4×10^{-3} °C/year and high temperatures for $< ca$ 0.5 Ma. The calculated peak temperature for each depth is nearly equal to the petrologically estimated value for each correlated metamorphic zone. The results suggest that the magma-intrusion model is one possible thermal model for low-pressure facies series metamorphism.

Key words: granitoid, low-pressure facies series metamorphism, magma-intrusion model, Ryoke metamorphic belt, temperature–time path, thermal modeling.

INTRODUCTION

Low-pressure facies series metamorphic belts are formed under P–T conditions that pass below the aluminosilicate triple point (~4 kbar), and the peak temperature ranges from 500 to 800 °C (Miyashiro 1961; De Yoreo *et al.* 1991). Such anomalously high temperatures at relatively shallow depth indicate that the geothermal gradient in the upper crust exceeds 50 °C/km at the time of low-P metamorphism. Many processes can generate a low-pressure facies series metamorphism (cf. De Yoreo *et al.* 1991; Takeshita & Okudaira 1994), including intrusion of igneous rocks, crustal extension, convective thinning of the mantle lithosphere, subduction of a young oceanic plate or spreading ridge, rapid uplift of doubled continental crust, increased heat flux from the mantle at the base of the crust, and advective heat transport by hot aqueous fluids. However, the close association between low-P metamorphism and magmatic activity in both space and time at many low-P metamorphic terranes suggests that intrusion of igneous rocks is a most likely cause for low-P metamorphism (De Yoreo *et al.* 1991). Numerical simulations for thermal evolution of the magmatic terranes show that magma intrusion can produce low-P metamorphism (Wells 1980; Lux *et al.* 1986; Hanson & Barton 1989; Rothstein & Hoisch 1994).

The Ryoke metamorphic belt of southwestern Japan (Fig. 1a) is mainly composed of Cretaceous Ryoke granitoids and associated metamorphic rocks of low-pressure facies series, and has been regarded as a typical example of low-P metamor-

*Present address: Geological Institute, University of Tokyo, 7-3-1 Hongo, Tokyo 113, Japan.

Accepted for publication April 1996.

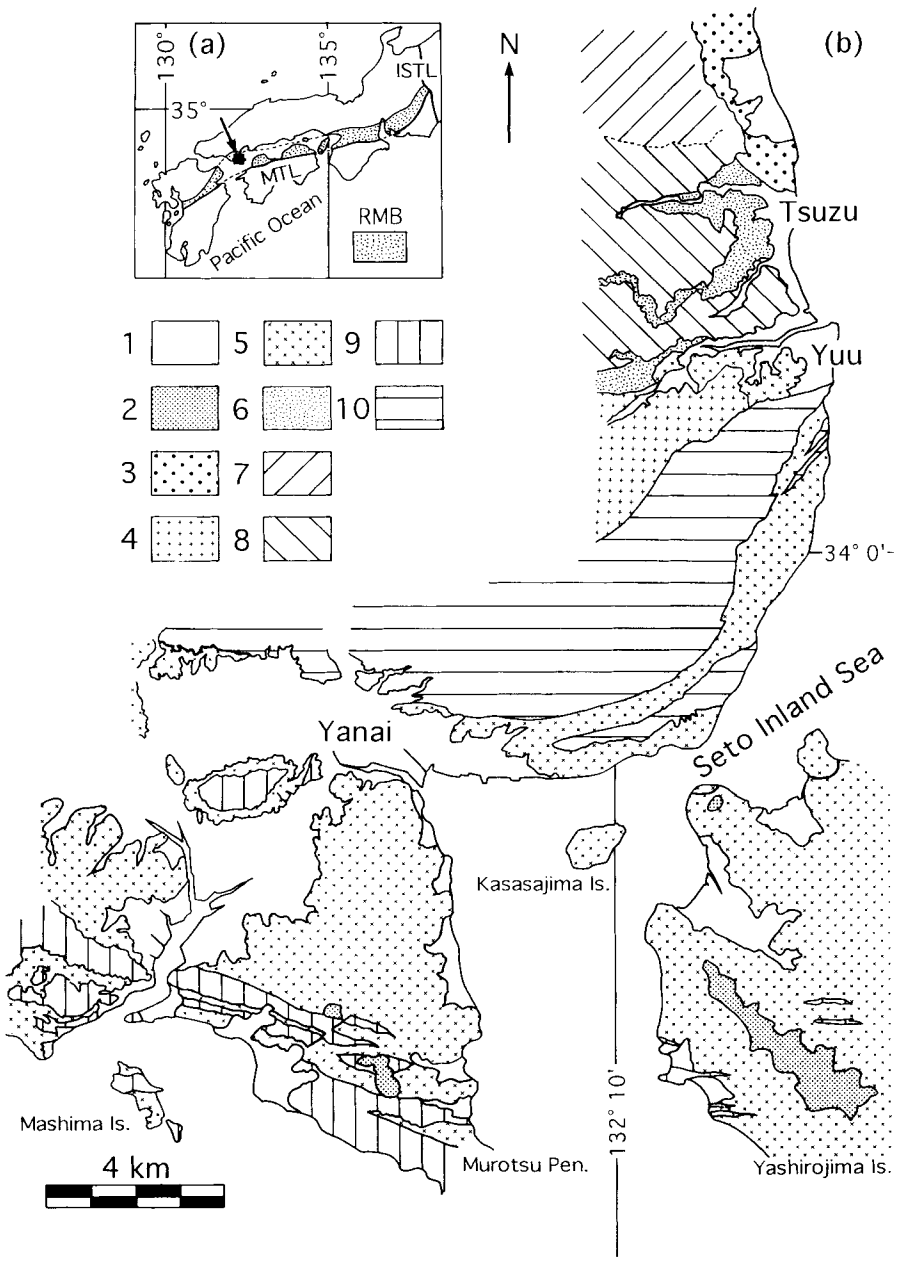

Fig. 1 (a) Map showing the location of the Ryoke metamorphic belt of southwestern Japan. RMB: Ryoke metamorphic belt; MTL: Median Tectonic Line; and ISTL: Itoigawa–Shizuoka Tectonic Line. (b) Geological and metamorphic zonation map of the Yanai district, southwestern Japan. 1, alluvium; 2, Tertiary volcanics; 3, Iwakuni granite; 4, Kibe granite; 5, Gamano granodiorite; 6, Tengatake–Nagano migmatite; 7–10, Ryoke metamorphic rocks (7, biotite zone; 8, cordierite zone; 9, sillimanite zone; 10, garnet zone).

phic belt (Miyashiro 1961; Banno & Nakajima 1992). The Ryoke granitoids have been divided into the sill-like Older Ryoke granitoids and the stock-like Younger Ryoke granitoids (Hara *et al.* 1991; Okudaira *et al.* 1993). The former intruded concordantly into the high-grade metamorphic rocks without development of a contact aureole, but the latter intruded discordantly into the low- to medium-grade metamorphic rocks with distinct contact aureoles.

In this paper the features of deformation and metamorphism in the Ryoke metamorphic belt in the Yanai district (Fig. 1b) will be described, and a possible thermal model for the low-pressure facies series metamorphism proposed. Mineral abbreviations used here are after Kretz (1983).

OUTLINE OF GEOLOGY

In the Yanai district (Fig. 1b) the Ryoke metamorphic belt mainly consists of the Gamano granodiorite, Tengatake-Nagano migmatite, Kibe granits, Iwakuni granite, and Ryoke metamorphic rocks of Cretaceous age (Nureki 1960; Okamura 1960; Kojima & Okamura 1968; Higashimoto *et al.* 1983; Okudaira *et al.* 1993, 1995). The Gamano granodiorite is mainly composed of hornblende–biotite

tonalite and hornblende-bearing biotite granodiorite, and is the most widely occurring Older Ryoke granitoid in the district. The Gamano granodiorite concordantly intruded into the high-grade metamorphic rocks at *ca* 95–100 Ma (Nakajima *et al.* 1993; Suzuki *et al.* 1994), and its foliation defined by the preferred shape orientation of plagioclase, biotite and hornblende is harmonic in trend with that of the surrounding metamorphic rocks. Geochemical evidence (Kagami *et al.* 1992) suggests a lower crustal and/or upper mantle origin for the Gamano granodiorite magma. The well-foliated granodiorite in the northern part of Yashirojima Island has been considered to be a fragment of the basement rocks to the Upper Paleozoic geosyncline in the inner side of southwestern Japan (Kojima & Okamura 1968). However, because the geochemical characteristics and CHIME monazite ages of the granodiorite are similar to those of the Gamano granodiorite (cf. Honma & Sakai 1975; Shigeno & Yamaguchi 1976; Suzuki *et al.* 1994), the two are correlated as part of the same body in this paper.

The Ryoke metamorphic rocks are mainly derived from pelites, psammites and cherts, with subordinate amounts of calcareous and basic rocks, which are considered to belong to the Jurassic accretionary complex (Kuga Group: cf. Higashimoto *et al.* 1983). These protoliths were regionally metamorphosed under low-pressure facies series conditions (M1) during the Early Cretaceous (*ca* 98 Ma: Suzuki *et al.* 1994). After the regional M1 metamorphism, the stock-like intrusions (Kibe and Iwakuni granites) distributed in the northern part of the studied area caused contact metamorphism in the surrounding rocks (Nureki *et al.* 1992; Okudaira *et al.* 1993, 1995). The contact metamorphic overprint is referred to as M2.

DEFORMATION STRUCTURES

LARGE-SCALE STRUCTURES

The Older Ryoke granitoids and metamorphic rocks were folded together in the district, and they can be divided into three structural domains: the northern, central and southern domains (Okudaira *et al.* 1993). Figure 2 shows the structural division and axial traces of major folds. The geological structure of the northern domain is characterized by gentle upright folds with the fold axis gently plunging toward east-southeast. The geological structure of the southern domain is also characterized by gentle folds of upright fashion and a west-northwest–east-southeast to east–west trend. In contrast to the structures of the northern and southern domains, the geological structure of the central domain is characterized by overturned folds facing toward the southeast direction with north-northeast–northeast plunging fold axes. Although the boundaries among the structural domains can be recognized in the limited areas, the boundaries may have an east–west strike and a northward dip (Fig. 2).

DEFORMATION EVENTS

In the Older Ryoke granitoids and metamorphic rocks, deformation structures caused by three different phases (D1, D2 and D3) of ductile deformation have been recognized (Okudaira *et al.* 1993, 1995). Deformation structures resulting from D1 and D3 are commonly observed, while the occurrence of the D2 structure is limited.

In all the rocks, D1 structure is characterized by a distinct foliation (S1-foliation) parallel to lithologic boundaries. In some metapelites, there are many kinds of asymmetric deformation structures: intrafolial folds (F1-folds) with axial planes parallel to S1-foliation (Fig. 3a); slightly rotated boudins of quartzo-feldspathic veins and thin layers of metachert (Fig. 3b); and extensional crenulation cleavages, rotated porphyroblasts and melt-filled R_1-fractures. Judging from the asymmetric structures, the overall movement picture of D1 is top to the north (Okudaira *et al.* 1995). The emplacement of the Older granitoids, for example the Gamano granodiorite and Tengatake-Nagano migmatite, occurred at least in part during D1, since the deformation structures of the granitoids are compatible with those of surrounding metamorphic rocks and granitoids injected into the R_1- and Y-fractures of the metamorphic rocks (Okudaira *et al.* 1995).

D2 is related to the formation of the large-scale overturned folds and their parasitic folds (F2-folds) which are facing toward the southeast with north-northeast–northeast plunging fold axes in the central domain, and to distinct shear zones (D2-shear zones) truncating S1-foliation (Fig. 3c,d). D2-shear zones are well observed near the boundary between the central and southern domains, but are not clear near the boundary between the northern and central domains. In the northern part of Yashirojima Island, in which the boundary between the central and southern domains is located, many fine-grained layers with distinct foliation (S2-foliation) are recognized as D2-shear zones truncating S1-foliation

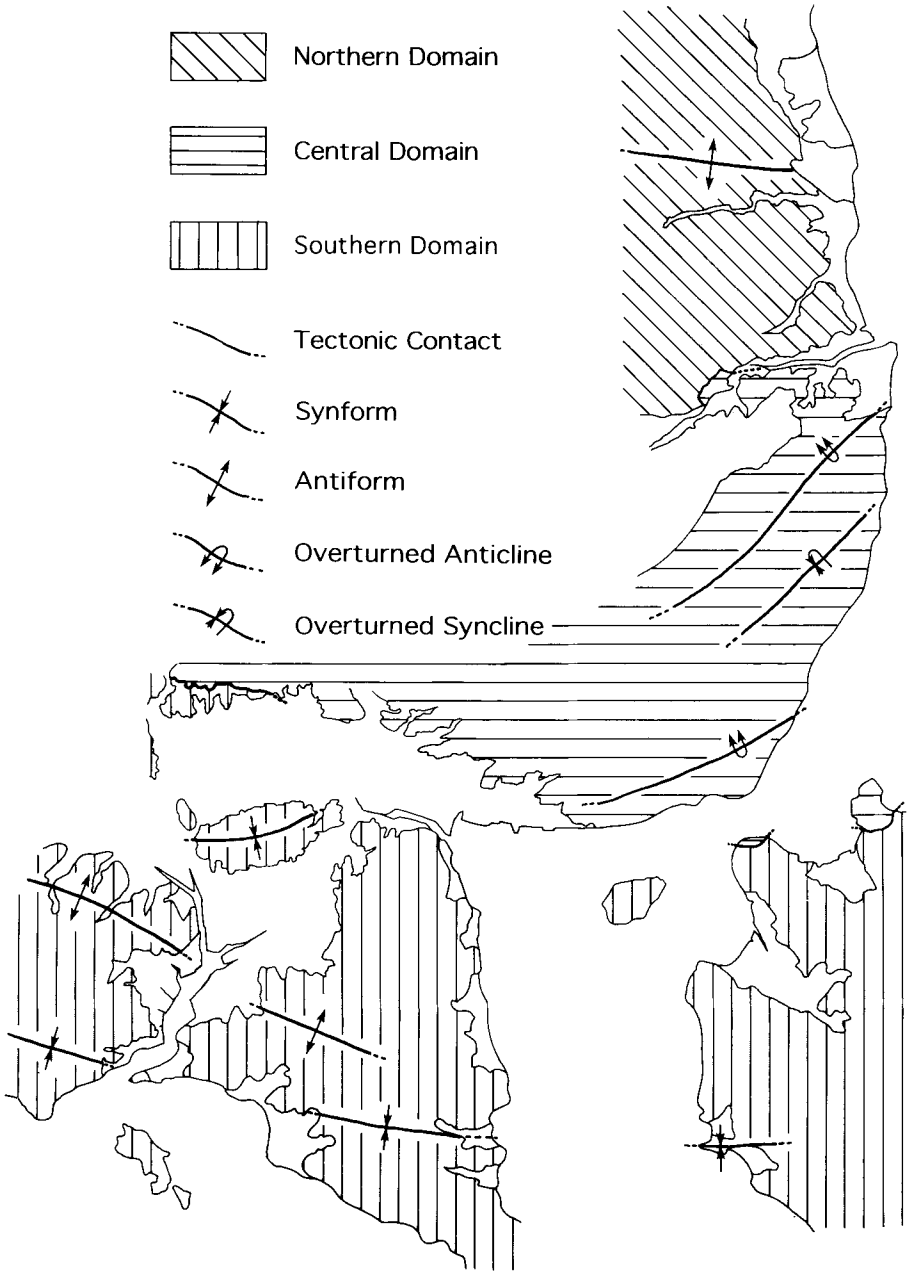

Fig. 2 Structural domains (northern, central and southern domains) in the Yanai district. Axial traces of major folds are also illustrated.

in the coarse-grained granodiorite (Fig. 3c). The fine-grained layers consist of grains (e.g. quartz and feldspar) produced by dynamic recrystallization of constituent minerals of the coarse-grained granodiorite (Sakurai & Hara 1990). The asymmetric structures (Fig. 3c,d) in the D2-shear zones near the boundary between the central and southern domains indicate the shear sense of top to the west-southwest–southwest.

D3 is responsible for the formation of gentle upright folds (F3-folds) with east–west-trending axes. D1 and D2 structures are folded by these F3-folds. The upright folds are correlated with upright folds developed in left-hand fashion throughout the Paleozoic-Mesozoic accretionary complexes in the Inner Zone of southwestern Japan (Hara *et al.* 1980, 1991).

REGIONAL METAMORPHISM

LOW-PRESSURE FACIES SERIES METAMORPHISM (M1)

The zonation of the Ryoke metamorphic rocks in the Yanai district has been proposed by many authors (Higashimoto *et al.* 1983; Ikeda 1991, 1993; Nureki *et al.* 1992; Okudaira *et al.* 1993, 1995; Nakajima 1994). The zonation in the previ-

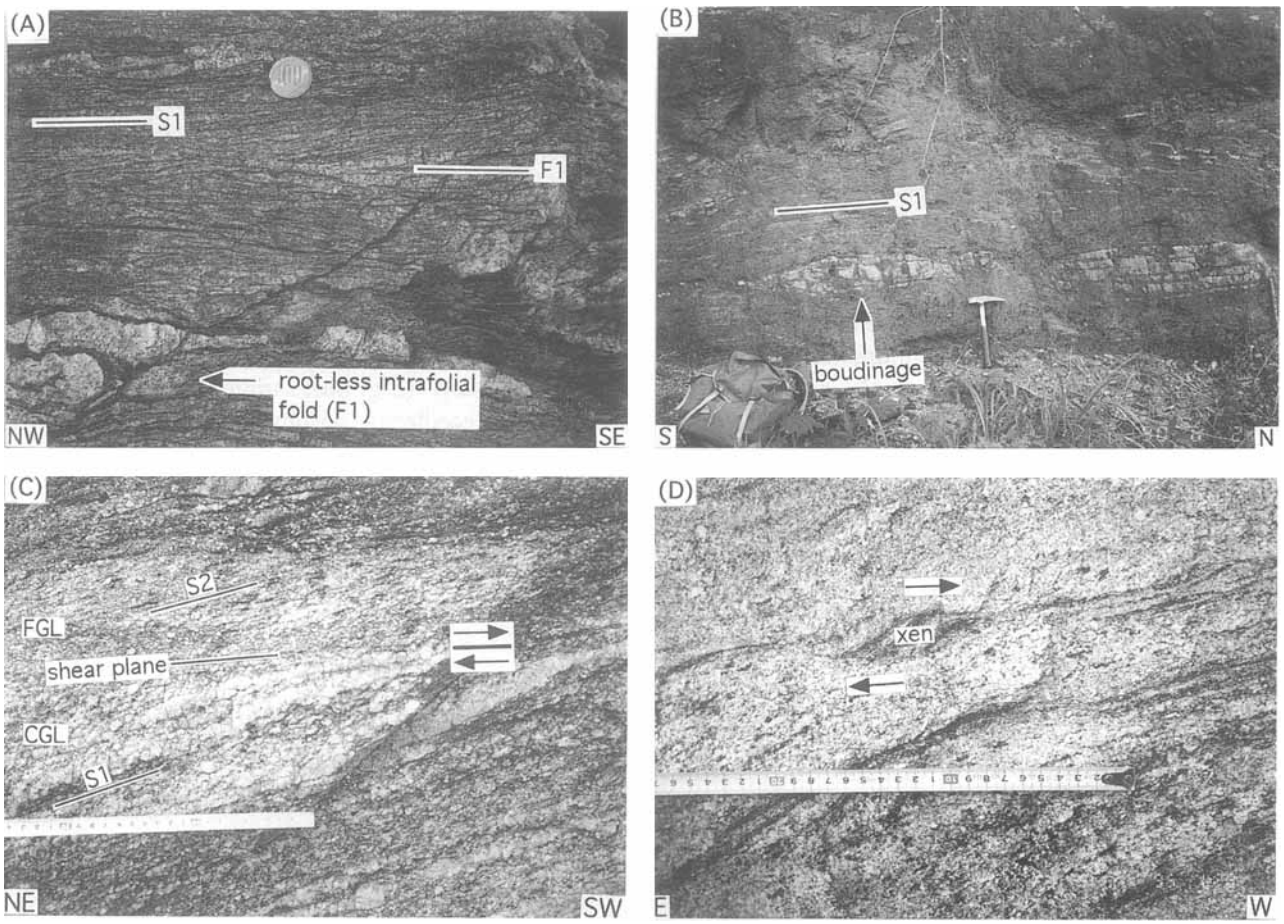

Fig. 3 D1 and D2 deformation structures on outcrop scale. (a) Intrafolial F1-folds (F1) with fold axis parallel to S1-foliation (S1). (b) Boudins of thin layers of metachert. (c) Fine-grained layer (FGL) caused by dynamic recrystallization of α coarse-grained layer (CGL) is recognized as D2-shear zones. S1 and S2 represent trends of foliation of a coarse-grained layer and a fine-grained layer, respectively. Arrows indicate the direction of shear along the shear plane related to D2-shear zone. (d) Asymmetrically elongated metabasic xenolith (xen) in the fine-gained layer. Arrows indicate the direction of shear inferred from the asymmetric structures.

ous studies is essentially similar. In Okudaira *et al.* (1993) and this study, on the basis of the mineral assemblages of minerals excluding inclusions in porphyroblasts in pelitic and psammitic rocks, the metamorphic rocks are divided into four metamorphic zones: biotite, cordierite, sillimanite and garnet. The distribution of these zones is shown in Fig. 1(b). The distributions of the biotite and cordierite zones, the sillimanite zone, and the garnet zone are restricted to the northern, southern, and central structural domains, respectively (see Figs 1b,2). The constituent phases of the pelitic and psammitic rocks are schematically shown in Fig. 4, and the typical mineral assemblages, excluding inclusion minerals in porphyroblasts, are the biotite zone: biotite + muscovite; cordierite

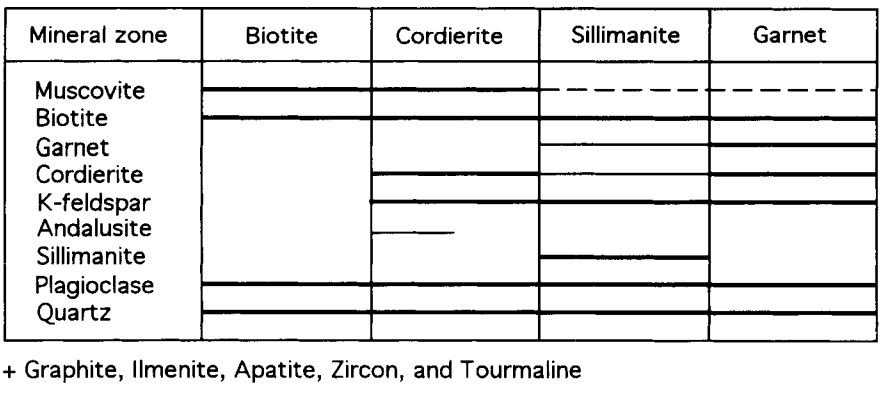

Fig. 4 Stability range of major constituent minerals of pelitic and psammitic rocks. ▬, ubiquitous phases; ——, reduced number of phases; and – – –, retrograde phases.

zone: biotite + muscovite + K-feldspar + cordierite ± andalusite; sillimanite zone: biotite + K-feldspar + sillimanite + garnet or cordierite; and the garnet zone: biotite + K-feldspar + cordierite + garnet; where all assemblages include quartz and plagioclase. Graphite, ilmenite, apatite, zircon and tourmaline occur as minor minerals. The first appearance of cordierite and K-feldspar defines the start of the cordierite zone. Andalusite occurs in the northern part of the cordierite zone. The sillimanite zone is defined by the occurrence of sillimanite as the only stable aluminosilicate mineral in the matrix. Garnet is often found, but does not coexist with cordierite in rocks of the sillimanite zone. The garnet zone is defined by the paragenesis of garnet and cordierite. In the garnet zone, sillimanite is not recognized as a matrix mineral, but is recognized as inclusions within cordierite and garnet porphyroblasts. In the sillimanite and garnet zones, muscovite is not a stable mineral at the thermal peak of M1, but occurs as a retrograde mineral, as muscovite grains do not form S1-foliation which is defined by preferred orientation of the minerals crystallized under M1.

Textural features observed in pelitic and psammitic rocks of the cordierite and garnet zones indicate some prograde metamorphic reactions. In the cordierite zone, cordierite and K-feldspar usually occur as porphyroblasts. The cordierite and K-feldspar porphyroblasts mainly include biotite, muscovite and quartz, which show distinct alignment as S0-foliation. The S0-foliation within the K-feldspar porphyroblasts is not commonly parallel to S1-foliation (Fig. 5a), while the S0-foliation within the cordierite porphyroblasts is commonly parallel to S1-foliation (Fig. 5b). The occurrences of biotite, muscovite and quartz within cordierite and K-feldspar porphyroblasts indicate the following prograde reaction (Massonne & Schreyer 1987):

$$\text{biotite} + \text{muscovite} + \text{quartz} = \text{cordierite} + \text{K-feldspar} + H_2O$$

The prograde P–T path of the cordierite zone

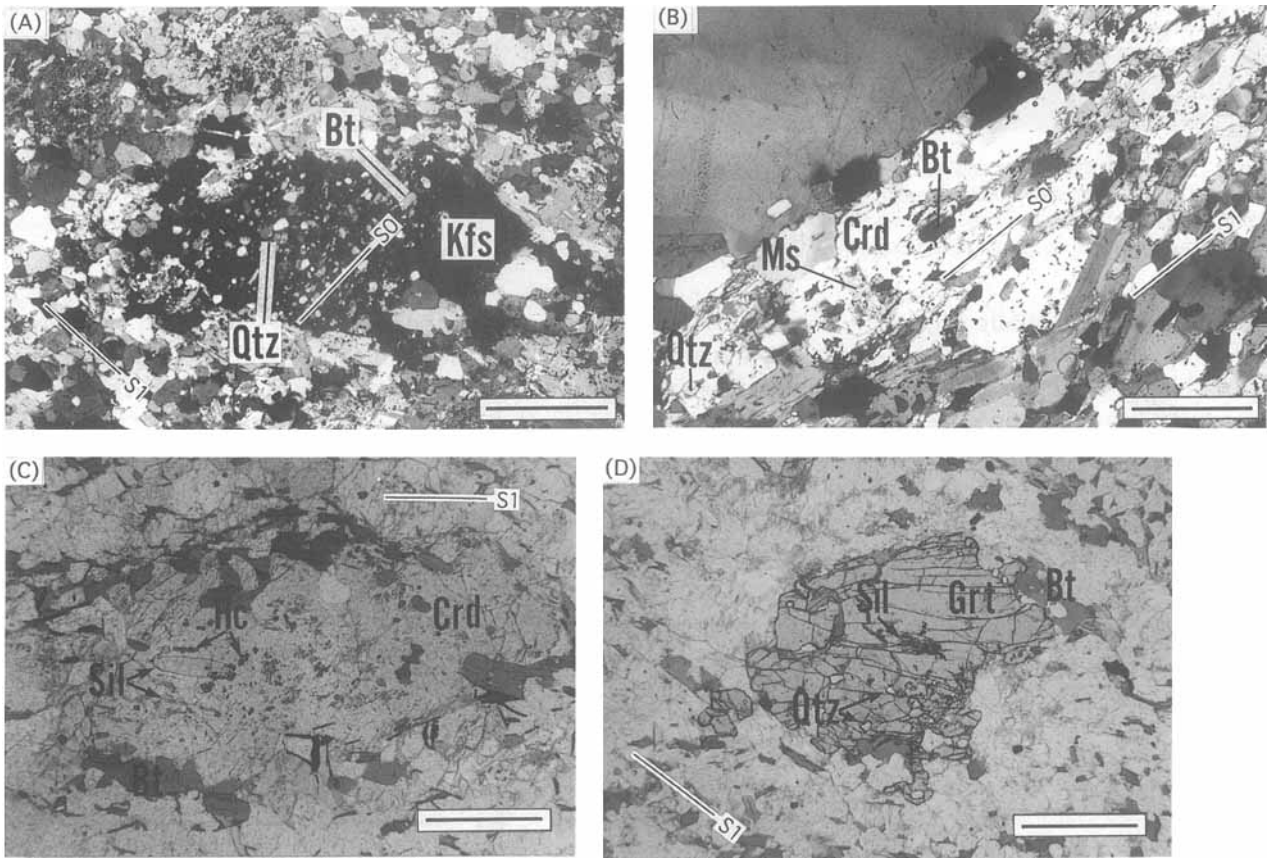

Fig. 5 Photomicrographs showing some relationship between inclusions and matrix minerals in pelitic and psammitic rocks of the cordierite and garnet zone. (a) K-feldspar porphyroblast containing quartz and biotite as an inclusion, which form S0-foliation truncated by S1-foliation. Scale bar is 0.5 mm. Crossed polars. (b) Cordierite porphyroblast containing quartz, biotite and muscovite as an inclusion, which form S0-foliation parallel to S1-foliation. Scale bar is 0.5 mm. Crossed polars. (c) Cordierite porphyroblast with inclusion biotite, sillimanite and hercynite, which form S0-foliation parallel to S1-foliation. Scale bar is 1 mm. Plane-polarized light. (d) Garnet porphyroblast with inclusion quartz and sillimanite. Scale bar is 1 mm. Plane-polarized light.

probably intersects the reaction. On the other hand, because muscovite has been a stable mineral in the zone, the prograde P–T path does not exceed the breakdown reaction of muscovite + quartz. In the garnet zone, cordierite and garnet occur as porphyroblasts. The cordierite porphyroblasts mainly include biotite, quartz and sillimanite with a small amount of hercynite and garnet. These inclusion minerals show a faint alignment as S0-foliation which is parallel to S1-foliation (Fig. 5c). The garnet porphyroblasts mainly contain quartz, graphite, ilmenite, biotite and sillimanite, which show no distinct alignment (Fig. 5d). The occurrences of biotite, sillimanite and quartz within the cordierite and garnet porphyroblasts indicate the following prograde reaction (Holdaway & Lee 1977):

$$\text{biotite} + \text{sillimanite} + \text{quartz} = \text{cordierite} + \text{K-feldspar} + \text{garnet} + H_2O$$

Pressure and temperature estimates

The minerals in metapelites crystallized under M1 are chemically analyzed to estimate the P-T conditions for the thermal peak of M1. Garnet crystals with a radius smaller than ~0.4 mm in the sillimanite zone and most of the garnet grains in the garnet zone show compositional zoning which consists of an unzoned core and reversely-zoned rim (Okudaira *et al.* 1993; Okudaira 1996). The material in the unzoned core probably crystallized near the peak metamorphic conditions, while that of the reversely-zoned rim was re-equilibrated during retrograde metamorphism (Okudaira 1996). In contrast, biotite, cordierite and plagioclase show no compositional zoning. However, biotite shows a local variation in the Ti content from grain to grain within one thin section (Ikeda 1991). Ikeda (1991) has suggested that biotite with low-Ti content was synchronously associated with the formation of reverse zoning in garnet during retrograde metamorphism. Therefore, the peak P–T conditions in the sillimanite and garnet zones would be estimated by using the compositions of the unzoned cores of garnet, cordierite, plagioclase, and biotite which is not in contact with garnet and has a high-Ti content. In this study, garnet-biotite (Thompson 1976; Holdaway & Lee 1977; Perchuk 1977) and two-feldspar (Stormer 1975; Stormer & Whitney 1977; Haselton *et al.* 1983) geothermometers are used for temperature estimation, and garnet-cordierite (Aranovich & Podlesskii 1983) and garnet-aluminosilicate-quartz-plagioclase (GASP; Hodges & Spear 1982) geobarometers are used for pressure estimation. The calculated P–T conditions are given in Tables A1, A2 and A3, and are summarized as the cordierite zone, 460 to 590°C; the sillimanite zone, 620–700°C at 3.0–4.5 kbar; and the garnet zone, 720–770°C at 5.5–6.5 kbar. Although pressure condition of the cordierite zone cannot be precisely estimated, it could be less than 4 kbar, probably about 3 kbar, because of the occurrence of andalusite. The metamorphic field gradient of M1 is ~40–50°C/km.

THERMAL MODELING FOR M1 METAMORPHISM

TECTONIC MODELING

As described in the preceding pages, the low-P metamorphism (M1) has a strong space and time association with emplacement of the Gamano granodiorite, as inferred from three lines of geological evidence as follows: (i) the granodiorite has been intruded into the high-grade metamorphic rocks during D1; (ii) throughout the high-grade metamorphic zones, distinct contact aureoles caused by the intrusion of the granodiorite are lacking; and (iii) intrusion ages (*ca* 95–100 Ma) of the granodiorite are similar to the ages of the thermal peak of M1 (*ca* 98 Ma). These geological observations suggest that M1 resulted from the intrusion of the Gamano granodiorite during D1.

The metamorphic zones are arranged, in order of increasing structural level, from biotite to cordierite to garnet to sillimanite. In contrast, the peak metamorphic temperature at M1 increases from the biotite zone, through the cordierite and sillimanite zones, to the garnet zone. The order of increasing metamorphic grade does not agree with the order of increasing structural level. The peak metamorphic conditions of the cordierite zone are significantly lower than those of the garnet zone by at least ~130°C and 2 kbar, and the higher pressure garnet zone structurally overlies the lower pressure sillimanite zone. This inverted thermal structure can be explained by large-scale faulting after the thermal peak of M1. In fact, S1-foliation, which is defined by the preferred orientation of the minerals crystallized under the thermal peak of M1, is truncated by the D2-shear zone that may be formed at the time of the large-scale faulting. Furthermore, the geological structures among the biotite and cordierite zones (northern domain), the garnet zone (central domain) and the sillimanite zone (southern domain) are significantly different, and the D2-shear zones are observed near the boundaries between the structural domains, which

may be developed on the upper and lower limbs of the large-scale D2-overturned folds. When the large-scale D2- and D3-folds are unfolded to flat-lying state, the Gamano granodiorite is underlain by the rocks of the garnet zone and overlain by the rocks of the sillimanite zone (Okudaira *et al.* 1993).

From these circumstances, a possible tectonic model for the Ryoke metamorphic belt in the district has been proposed by Okudaira *et al.* (1993), as shown in Fig. 6. The tectonic model is considered to be as follows: (i) the low- to flat-angle intrusion of the Gamano granodiorite during D1 resulted in M1 (Fig. 6a); and (ii) after D1 the metamorphic sequence of M1 was modified by the deformation during D2 and D3 (Fig. 6b). According to the tectonic model, to clarify the thermal effects of the emplacement of the Gamano granodiorite, I propose a simple thermal model for M1, using a 1-D numerical simulation.

NUMERICAL MODELING

Numerical methods

A one-dimensional heat transfer equation can be written as

$$\rho_m C_m \frac{\partial T}{\partial t} = K \frac{\partial^2 T}{\partial z^2} + A \qquad (1)$$

Where ρ_m = density of rock (2750 kg/m^3); C_m = specific heat of rock (880 J/kg·K); T = temperature (K); t = time (s); K = thermal conductivity (2.8 W/m·K); z = vertical coordinate measured from the earth's surface; and A is heat production of radioactive elements (W/m^3). Density and specific heat of magma are assumed to be similar to those of rock, according to Hanson and Barton (1989), Rothstein and Hoisch (1994), and others. Equation (1) was solved numerically using an explicit finite difference method with a 1000 m array spacing (Δz) and a 3.15×10^9 s time step (Δt).

Production of heat during the crystallization of magma (i.e. latent heat), and consumption of heat by the endothermic reactions have been calculated by assuming reactions to be a continuous linear function of temperature between the crystallization interval ($T_{liq} - T_{sol}$) and between the endothermic reaction interval ($T_{end} - T_{start}$), respectively. Following Wells (1980) and Hanson and Barton (1989), I have used the crystallization intervals ($T_{liq} - T_{sol}$) of 750 and 950°C for the initial intrusion temperature (T_{int}) of 900°C for granodioritic composition, and taken the value of 3.35×10^5 J/kg for enthalpy (ΔH_{magma}) of crystallizing magma. In the crystallizing magma, recharge and convection are neglected.

In the wall rocks, most dehydration reactions are endothermic and thus consume heat (Peacock 1989). For typical dehydration reactions, enthalpy (ΔH_{rxn}) of the reactions is in the range of 60 to 100 kJ per mole of volatile evolved (Walther & Orville 1982). During metamorphism, a typical pelite loses approximately 5 wt% volatiles which is structurally bound in hydrous minerals (Walther & Orville 1982). This is equivalent to approximately 7.6×10^3 moles/m^3 of rock. Assuming 60 kJ/mole for dehydration reactions results in a heat sink of 1.7×10^5 J/kg (Peacock 1989). Since the actual metamorphic reactions are too complex to adequately calculate the thermal evolution, the continuous dehydration reaction between 350 and 800°C is modeled here. It is assumed that rocks initially at temperatures below 350°C and above 800°C contain 5 and 0 wt% volatiles, respectively. For rocks initially at the temperatures within the reaction interval, the volatile content (X_{fluid}) is calculated from the following equation:

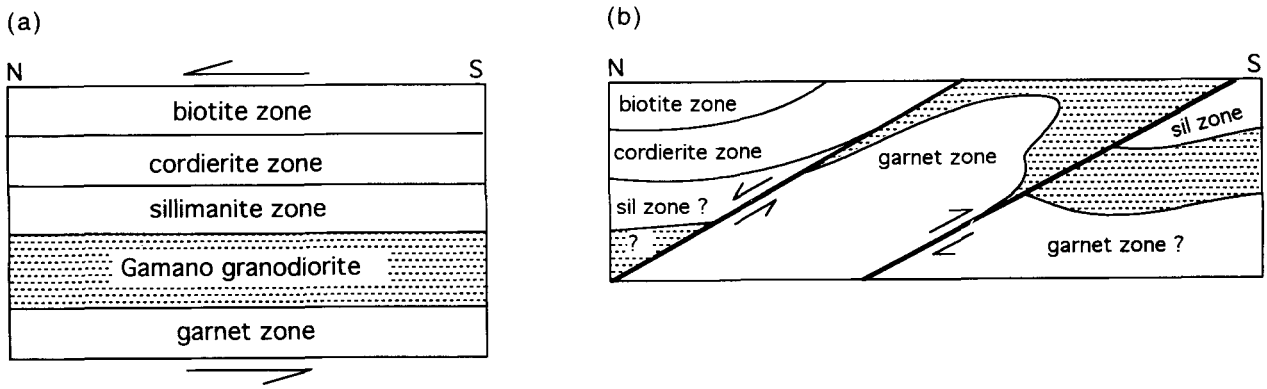

Fig. 6 Schematic geological configurations at (a) D1 and (b) D2 and D3 after Okudaira *et al.* (1993). See text for further details.

$$X_{\text{fluid}} = 0.05(T_{\text{end}} - T)/(T_{\text{end}} - T_{\text{start}}), \quad T_{\text{start}} < T < T_{end} \tag{2}$$

The initial volatile content in the wall rocks is illustrated in Fig. 7b.

The production and consumption of heat were incorporated into the numerical model using an effective heat capacity, C^*, and an effective thermal diffusivity, κ^*, for rock undergoing the reactions (Jaeger 1964; Peacock 1989; Hanson & Barton 1989). The effective thermal diffusivity is then calculated from

$$\kappa^* = \frac{K}{\rho_m C^*}, \tag{3}$$

where the effective heat capacity (C^*) is defined by

$$C^* = C_m + [\Delta H_{\text{magma}}/(T_{\text{liq}} - T_{\text{sol}})] \tag{4a}$$

for the magmatic crystallization, and

$$C^* = C_m + [\Delta H_{\text{rxn}}/(T_{\text{end}} - T_{\text{start}})] \tag{4b}$$

for metamorphic endothermic reactions.

The radiogenic heat production (the second term on the right side of Equation (1)) of decaying elements decreases exponentially with depth according to the relation (Turcotte & Schubert 1982):

$$A = A_0 e^{-z/h_r} \tag{5}$$

where A_0 and h_r are the surface radiogenic heat production (2.60×10^{-6} W/m^3) and the characteristic length scale (10 km), respectively. On the other hand, for the magma, the heat production resulting from the decay of radioactive elements, A, is represented by that of magma A_g (2.64×10^{-6} W/m^3).

The initial continental geotherm immediately before the intrusion of magma is calculated from (Turcotte & Schubert 1982):

$$T_i = T_s + \frac{q_m z}{K} + \frac{A_0 h r^2}{K}(1 - e^{-z/h_r}) \tag{6}$$

where T_i, T_s and q_m are the initial temperature of the rock, the surface temperature and the mantle heat flux, respectively. In this study, the boundary conditions are constant temperature (0 °C) at $z = 0$ and constant mantle heat flux, q_m, at the bottom of the lithosphere. The thickness of the lithosphere before the intrusion of the Gamano granodiorite is assumed to be 30 km, because the thickness of the mechanical lithosphere beneath a typical island arc has been estimated to be ~20 to 30 km based on rheology of the constituent minerals of the lithosphere (Shimamoto 1994). Since the mean geothermal gradient of an active continental margin or island arc is ~30 °C/km (Sugimura & Uyeda 1973), the initial geotherm in the lithosphere was set to be ~30 °C/km and then q_m would be assumed to be 0.08 W/m^2.

According to the relation $z = P$ (in Pa)$/(\rho_m \cdot g)$, the depths of the sillimanite and garnet zones were estimated to be ~15 km ($P = 0.4$ GPa) and 20 km ($P = 0.55$ GPa) respectively, and then a 3 km-thick sheet-like intrusion between 16 and 19 km in depth was assumed. The emplacement of the Gamano granodiorite was modeled as an instantaneous and a single intrusion. The instantaneous pluton emplacement can be assumed to simplify the model, because theoretical studies suggest that magmas rise quickly relative to their rate of cooling (cf. Rothstein & Hoisch 1994). After the intrusion, the thickness of the lithosphere instantaneously inflates to 35 km. Figure 7(a) shows initial and boundary conditions for the thermal model for M1.

Results of the simulation

Figure 8 shows the temperature–depth curves with increasing time. Thermal relaxation of the situation shown in Fig. 7(a) is fast. Figure 9 gives temperature–time (T–t) paths at three depth levels

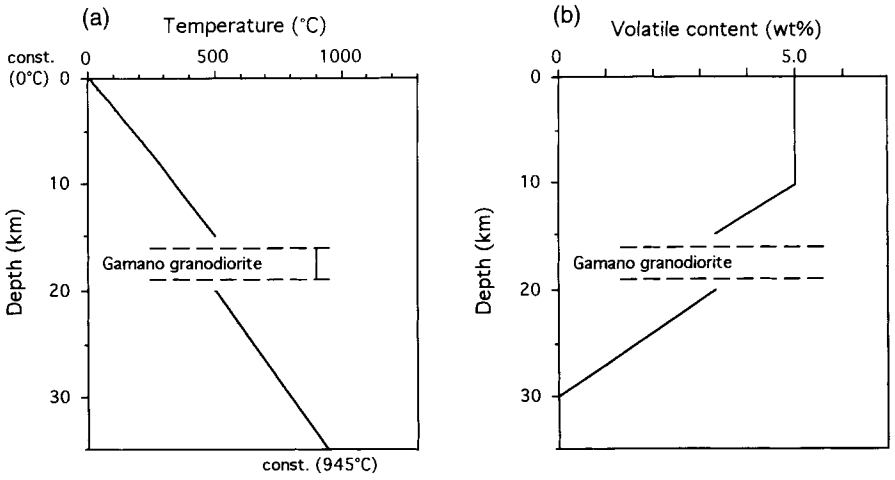

Fig. 7 (a) Initial and boundary conditions for the 1-D thermal model for M1. (b) Initial volatile contents of the wall rocks as a function of depth.

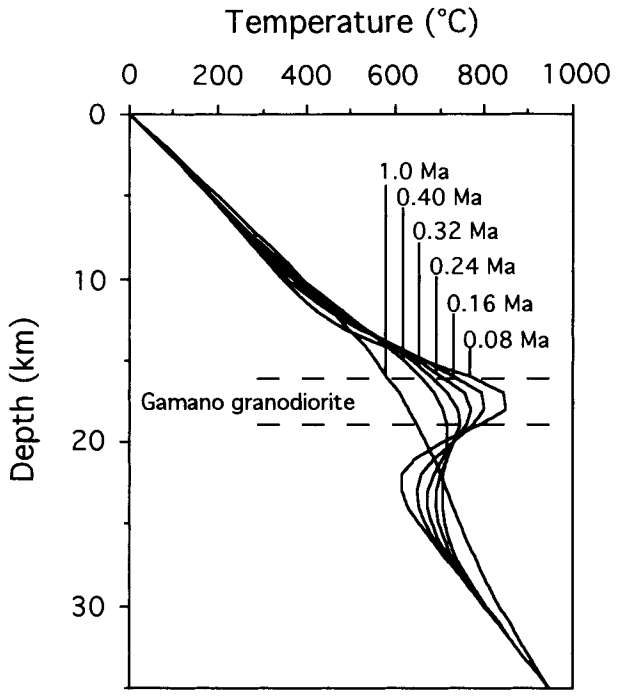

Fig. 8 Temperature-depth curves showing thermal evolution of the 35-km-thick lithosphere immediately after instantaneous intrusion of the Gamano granodiorite.

(12, 15 and 20 km) associated with the situation in Fig. 7(a), and the petrologically estimated peak metamorphic temperatures are also drawn as stippled parts. At the 12 km depth point, which is probably correlated with the cordierite zone, the peak temperature reaches 480 °C at 0.4 Ma in the system's evolution (Fig. 9a). The average rate of temperature increase is $\sim 0.2 \times 10^{-3}$ °C/year, and the period of a high-temperature condition (>450 °C) is shorter than ~1.4 Ma. The calculated peak temperature is well within the petrologically estimated peak temperatures between ~460 and 590 °C. At the depth point of 15 km, which is correlated with the sillimanite zone, the peak temperature reaches 670 °C at 0.12 Ma (Fig. 9b). The average rate of temperature increase is $\sim 1.4 \times 10^{-3}$ °C/year, and the period of a high-temperature condition (>600 °C) is shorter than 0.5 Ma. The calculated peak temperature is well within the petrologically estimated peak temperatures between ~620 and 700 °C. The peak temperature at the depth point of 20 km, which is correlated with the garnet zone, reaches 740 °C at 0.26 Ma (Fig. 9c). The average rate of temperature increase is $\sim 0.9 \times 10^{-3}$ °C/year, and the period of a high-temperature condition (>700 °C) is shorter than ~0.6 Ma. The calculated peak temperature is within the petrologically estimated peak temperatures between ~720 and 770 °C.

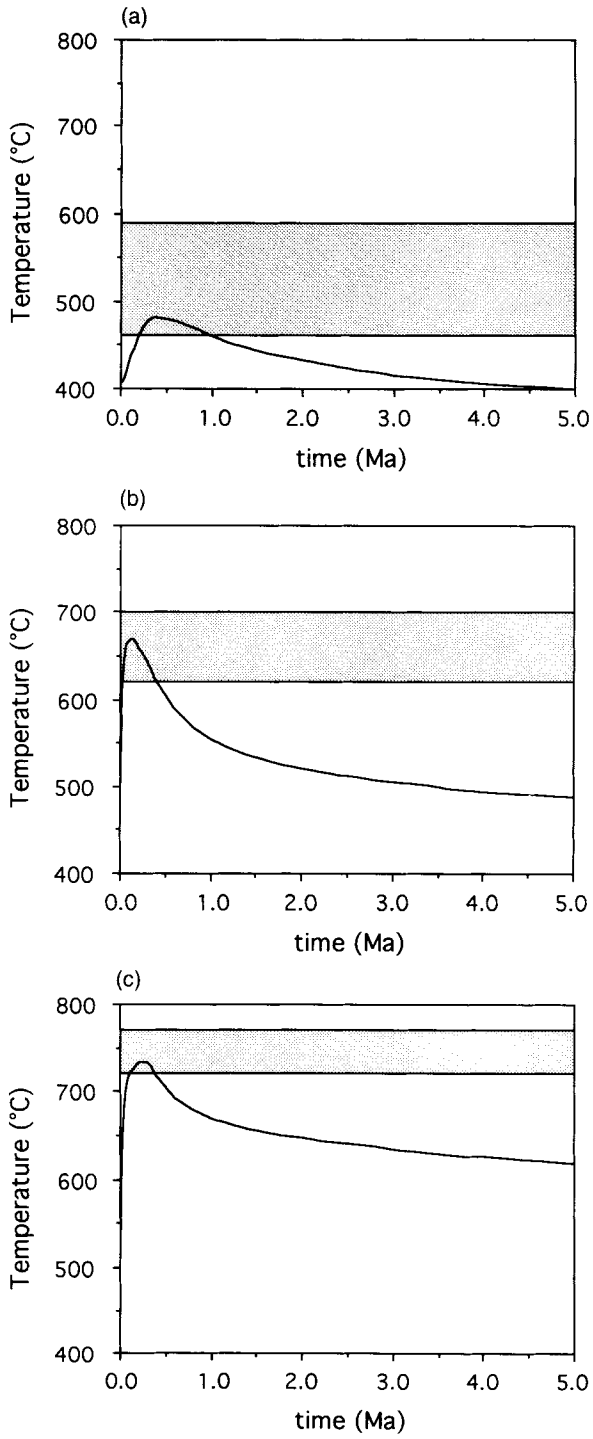

Fig. 9 Temperature-time plots at depths of (a) 12 km; (b) 15 km; and (c) 20 km. Each crustal level corresponds to the depths of the cordierite, sillimanite and garnet zones, respectively. ▨, petrologically estimated peak metamorphic temperatures.

In summary, the calculated peak temperature for each depth is nearly equal to the petrologically estimated value for each correlated metamorphic zone. These results suggest that the magma-

intrusion model is one of the possible thermal models for the low-pressure facies series Ryoke metamorphism.

EVALUATION OF THE NUMERICAL MODELING

Okudaira (1996) suggested that the validity of the metamorphic T–t path can be examined by using chemical zoning in garnet as described as follows. Garnet crystals from the rock of the sillimanite zone show various chemical zoning patterns. The zoning pattern at the core of the garnet grains systematically varies, with increasing grain size of the garnet, from reversely zoned, through unzoned, to normally zoned patterns. Quantitative and qualitative textural analyses of the garnet grains led to the conclusion that the crystallization mechanism for garnet grains between 0.1 and 0.5 mm radii was continuous nucleation and diffusion-controlled growth. Chemical zoning of garnet grains with different radii was simulated for the previously estimated T–t path for the sillimanite zone (Okudaira *et al.* 1994) (which is similar to the path of the sillimanite zone proposed here (Fig. 9b)) using a numerical model of continuous nucleation and diffusion-controlled growth, in combination with intracrystalline diffusion. The results of the simulation of Okudaira (1996) indicated that the observed zoning patterns of the various sizes of garnet were well reproduced by the numerical model, in spite of the fact that simulated zoning patterns strongly depended on T–t history, for example, the chemical composition of garnet changed according to subtle changes in temperature. Therefore, at least for the sillimanite zone, the T–t path proposed here gives a good explanation for the low-P Ryoke metamorphism.

However, there are some uncertainties in the thermal model, the most important being the initial temperature of each metamorphic zone because the initial geothermal gradient of the lithosphere cannot be precisely estimated by geological observations, and there is a large uncertainty in the depth (pressure) estimate of each metamorphic zone. This uncertainty leads to a different calculated highest temperature at each metamorphic zone. The difference of 1 kbar between the estimated and actual pressures leads to a difference of 3.7 km in their depth estimates. In the case of a linear geothermal gradient of 30°C/km, a depth of 3.7 km is equivalent to a temperature of 110°C, and leads to a difference of less than ~55°C in the calculated highest temperature at each metamorphic zone. Therefore, an accurate pressure estimate will be quite necessary for more refined thermal modeling in future.

SUMMARY

The Ryoke metamorphic belt in the Yanai district of southwestern Japan is mainly composed of sheet-like Gamano granodiorite and metamorphic rocks of low-pressure facies series. The Gamano granodiorite intruded into the high-grade metamorphic rocks without causing a distinct contact metamorphic overprint. From the analyses of deformation and metamorphism of the rocks, the low-P metamorphism was probably caused by the syn-deformational emplacement of the Gamano granodiorite. Furthermore, from the results of 1-D numerical modeling of the thermal effects of the emplacement of the Gamano granodiorite, the calculated peak temperature investigated at each depth (12, 15 and 20 km) is nearly equal to the petrologically estimated value for each metamorphic zone (cordierite, sillimanite and garnet). The geological observations and simulated results suggest that the low-pressure facies series metamorphism in the Yanai district largely resulted from the intrusion of the Gamano granodiorite.

ACKNOWLEDGEMENTS

I express my sincere thanks to I. Hara, Y. Hayasaka and T. Takeshita for constructive comments and critical readings of the early version of the manuscript. The paper benefited substantially from detailed reviews by M. Brown, T. Ikeda, M. Komatsu and T. Nishiyama. I also thank A. Minami for helpful assistance with the electron-probe analyses at the Instrument Center for Chemical Analysis, Hiroshima University. However, all responsibility for this paper is mine.

REFERENCES

ARANOVICH L. YA. & PODLESSKII K. K. 1983. The cordierite-garnet-sillimanite-quartz equilibrium: Experiments and applications. *In* Saxena S. K. ed. *Kinetics and Equilibrium in the Mineral Reactions, Advances in Physical Geochemistry* **3**, pp. 173–98. Springer-Verlag, New York.

BANNO S. & NAKAJIMA T. 1992. Metamorphic belts of Japanese Islands. *Annual Reviews in Earth and Planetary Sciences* **20**, 159–79.

DE YOREO J. J., LUX D. R. & GUIDOTTI C. V. 1991. Thermal modeling in low-pressure/high-temperature metamorphic belts. *Tectonophysics* **188**, 209–38.

HANSON R. B. & BARTON M. D. 1989. Thermal development of low-pressure metamorphic belts: Results from two-dimensional numerical models. *Journal of Geophysical Research* **94**, 10 363–77.

HARA I., SHOJI K., SAKURAI Y., YOKOYAMA S., & HIDE K. 1980. Origin of the median tectonic line and its initial shape. *Memoirs of Geological Society of Japan* **18**, 27–49.

HARA I., SAKURAI Y., OKUDAIRA T., HAYASAKA Y., OHTOMO Y. & SAKAKIBARA N. 1991. Tectonics of the Ryoke belt. *Excursion Guidebook of 98th Annual Meeting of Geological Society of Japan*, Geological Society of Japan, Matsuyama. pp. 1–20 (in Japanese).

HASELTON H. T., HOVIS G. L., HEMINGWAY B. S. & ROBIE R. A. 1983. Calorimetric investigation of the excess entropy of mixing in analbite-sanidine solid solution: Lack of evidence for Na, K short-range order and implications for two-feldspar thermometry. *American Mineralogist* **68**, 398–413.

HIGASHIMOTO S., NUREKI T., HARA I., TSUKUDA E. & NAKAJIMA T. 1983. *Geology of the Iwakuni District 1 : 50 000*. Geological Survey of Japan (in Japanese with English abstract).

HODGES K. V. & SPEAR F. S. 1982. Geothermometry, geobarometry and the Al_2SiO_5 triple point at Mt. Moosilauke, New Hampshire. *American Mineralogist* **67**, 1118–34.

HOLDAWAY M. J. & LEE S. M. 1977. Fe–Mg cordierite stability in high-grade pelitic rocks based on experimental, theoretical, and natural observations. *Contributions to Mineralogy and Petrology* **63**, 175–98.

HONMA H. & SAKAI H. 1975. Oxygen isotope study of metamorphic and granitic rocks of the Yanai district in the Ryoke belt, Japan. *Contributions to Mineralogy and Petrology* **52**, 107–20.

IKEDA T. 1991. Heterogeneous biotite from Ryoke metamorphic rocks in the Yanai district, southwest Japan. *Journal of Geological Society of Japan* **97**, 537–47.

IKEDA T. 1993. Compositional zoning patterns of garnet during prograde metamorphism from the Yanai district, Ryoke metamorphic belt, southwest Japan. *Lithos* **30**, 109–22.

JAEGER J. C. 1964. Thermal effects of intrusions. *Reviews of Geophysics* **2**, 44–54.

KAGAMI H., IIZUMI S., TAINOSHO Y. & OWADA M. 1992. Spatial variations of Sr and Nd isotope ratios of Cretaceous–Paleogene granitoid rocks, southwest Japan arc. *Contributions to Mineralogy and Petrology* **112**, 165–77.

KOJIMA G. & OKAMURA Y. 1968. On the Kitaoshima granite gneiss complex. *Journal of Hiroshima University, Series C* **5**, 295–306.

KRETZ R. 1983. Symbols for rock-forming minerals. *American Mineralogist* **68**, 277–9.

LUX D. R., DE YOREO J. J., GUIDOTTI C. V. & DECKER E. R. 1986. The role of plutonism in low-pressure/high-temperature metamorphic belt formation. *Nature* **323**, 794–7.

MASSONNE H. & SCHREYER W. 1987. Phengite geobarometry based on the limiting assemblage with K-feldspar, phlogopite, and quartz. *Contributions to Mineralogy and Petrology* **96**, 212–24.

MIYASHIRO A. 1961. Evolution of metamorphic belts. *Journal of Petrology* **2**, 277–311.

NAKAJIMA T. 1994. The Ryoke metamorphic belt: Crustal section of the Cretaceous Eurasian continental margin. *Lithos* **33**, 51–66.

NAKAJIMA T., WILLIAMS I. S. & WATANABE T. 1993. SHRIMP U-Pb ages of the Ryoke and San-yo granitoids in Southwest Japan. *Abstract with Programs, 100th Annual Meeting of Geological Society of Japan*, 584 (in Japanese).

NUREKI T. 1960. Structural investigation of the Ryoke metamorphic rocks of the area between Iwakuni and Yanai, Southwestern Japan. *Journal of Science of Hiroshima University, Series C* **3**, 69–141.

NUREKI T., ENAMI M., SHIOTA T. & SHIBATA T. 1992. Paired metamorphic belts: Ryoke and Sanbagawa. *29th IGC Field Trip Guide Book* **5**, 103–32.

OKAMURA Y. 1960. Structural and petrological studies on the Ryoke gneiss and granodiorite of the Yanai district, Southwest Japan. *Journal of Science of Hiroshima University, Series C* **3**, 143–213.

OKUDAIRA T. 1996. Temperature–time path for the low-pressure Ryoke metamorphism, Japan, based on chemical zoning in garnet. *Journal of Metamorphic Geology* **14**, 427–40.

OKUDAIRA T., HARA I., SAKURAI Y. & HAYASAKA Y. 1993. Tectono-metamorphic processes of the Ryoke belt in the Iwakuni-Yanai district, southwest Japan. *Memoirs of Geological Society of Japan* **42**, 91–120.

OKUDAIRA T., HARA I. & TAKESHITA T. 1994. Thermal modeling for the low-pressure facies series Ryoke metamorphism. *Earth Monthly* **16**, 486–9 (in Japanese).

OKUDAIRA T., HARA I. & TAKESHITA T. 1995. Emplacement mechanism of the Older Ryoke granites in the Yanai district, southwest Japan, with special reference to extensional deformation in the Ryoke metamorphic belt. *Journal of Science of Hiroshima University, Series C* **10**, 357–66.

PEACOCK S. M. 1989. Numerical constraints on rates of metamorphism, fluid production, and fluid flux during regional metamorphism. *Geological Society of America Bulletin* **101**, 476–86.

PERCHUK L. L. 1977. Thermodynamic control of metamorphic processes. *In* Saxena S. K. & Bhattacharji S. eds. *Energetics of Geological Processes*. pp. 285–352, Springer-Verlag, New York.

ROTHSTEIN D. A. & HOISCH T. D. 1994. Multiple intrusions and low-pressure metamorphism in the central Old Woman Mountains, south-eastern California: Constraints from thermal modelling. *Journal of Metamorphic Geology* **12**, 723–34.

SAKURAI Y. & HARA I. 1990. Deformation styles and tectonics of granitic rocks of the Ryoke belt (I) Deformation styles of plagioclase. *Earth Monthly* **12**, 457–61 (in Japanese).

SHIGENO H. & YAMAGUCHI M. 1976. A Rb–Sr isotopic study of metamorphism and plutonism in the Ryoke belt, Yanai district, Japan. *Journal of Geological Society of Japan* **82**, 687–98 (in Japanese with English abstract).

SHIMAMOTO T. 1994. Rheology of lithosphere: Current status and future perspectives. *Structural Geology* **39**, 147–52 (in Japanese with English abstract).

STORMER J. C. 1975. A practical two-feldspar geothermometer. *American Mineralogist* **60**, 667–74.

STORMER J. C. & WHITNEY J. A. 1977. Two-feldspar geothermometry in granulite facies metamorphic rocks. *Contributions to Mineralogy and Petrology* **65**, 123–33.

SUGIMURA A. & UYEDA S. 1973. *Island arcs, Japan, and its Environs. Development of Geotectonics* **3**, Elsevier, Amsterdam.

SUZUKI K., ADACHI M. & KAJIZUKA I. 1994. Electron microprobe observations of Pb diffusion in metamorphosed detrital monazites. *Earth and Planetary Science Letters* **128**, 391–405.

TAKESHITA T. & OKUDAIRA T. 1994. Dynamics and thermal modeling in low-pressure/high-temperature metamorphic belts. *Zisin (Journal of Seismological Society of Japan), Series 2* **47**, 453–67 (in Japanese with English abstract).

THOMPSON A. B. 1976. Mineral reactions in pelitic rocks 2: Calculation of some P-T-X (Fe–Mg) phase reactions. *American Journal of Science* **276**, 425–54.

TURCOTTE D. L. & SCHUBERT G. 1982. *Geodynamics*. John Wiley and Sons, New York.

WELLS P. R. A. 1980. Thermal models for the magmatic accretion and subsequent metamorphism of continental crust. *Earth and Planetary Science Letters* **46**, 253–65.

APPENDIX

Pressure and temperature estimates for the rocks of the cordierite, sillimanite and garnet zones. Metamorphic minerals were analyzed using an electron-probe microanalyzer (JEOL, JCMA-733II) at the Instrument Center for Chemical Analysis, Hiroshima University, operating at an accelerating voltage of 15 kV, a current of 19 nA and a beam width of 5 μm.

Table A1. Temperature estimates for the cordierite zone. Methods for temperature estimation are as follows: T1 = Stormer (1975); T2 = Stormer & Whitney (1977); T3 = Haselton *et al.* (1983). Temperature (°C) at 3 kbar.

Sample no.	X_{Na}^{Pl}	X_{Ca}^{Pl}	X_{Na}^{Kfs}	X_{K}^{Kfs}	T1	T2	T3
Z-51	0.743	0.249	0.090	0.909	445	490	425
F-8	0.749	0.236	0.133	0.865	503	553	501
E-23	0.732	0.258	0.120	0.878	491	539	485
E-7	0.737	0.251	0.156	0.842	535	589	546
S-1	0.807	0.183	0.161	0.830	517	573	509
F-11	0.610	0.379	0.142	0.856	566	616	589
F-13	0.759	0.231	0.179	0.820	552	612	569

Table A2. *P–T* estimates for the sillimanite zone. Methods for *P–T* estimation are as follows: T1 = Thompson (1976); T2 = Holdaway & Lee (1977); T3 = Perchuk (1977); P1 = Hodges & Spear (1982). Temperature (°C) at 4.0 kbar. Pressure (kbar) at 650°C.

Sample no.	X_{Fe}^{Grt}	X_{Mg}^{Grt}	X_{Ca}^{Grt}	X_{Mg}^{Bt}	X_{Ca}^{Pl}	T1	T2	T3	P1
911005-04	0.583	0.164	0.038	0.492	0.333	707	705	686	4.2
911113-04	0.657	0.112	0.032	0.440	0.253	614	624	618	4.7
911113-12	0.729	0.111	0.024	0.407	0.279	621	630	623	3.0
921106-10	0.595	0.121	0.028	0.462	0.239	640	647	637	4.4

Table A3. *P–T* estimates for the garnet zone. Methods for *P–T* estimation are as follows: T1 = Thompson (1976); T2 = Holdaway & Lee (1977); T3 = Perchuk (1977); P1 = Aranovich & Podlesskii (1983). Temperature (°C) at 5.5 kbar. Pressure (kbar) at 750°C.

Sample no.	X_{Fe}^{Grt}	X_{Mg}^{Grt}	X_{Ca}^{Grt}	X_{Mg}^{Bt}	X_{Mg}^{Crd}	T1	T2	T3	P1
900424-01	0.729	0.168	0.022	0.410	0.547	755	753	721	5.9
900510-04	0.700	0.190	0.021	0.433	0.560	783	777	740	6.4
910430-07	0.732	0.139	0.032	0.362	0.513	759	757	723	5.5
911114-01	0.716	0.178	0.027	0.444	0.581	732	733	704	6.0